Bose-Einstein condensate collapse and dynamical squeezing of vacuum fluctuations

E. A. Calzetta[1,*] and B. L. Hu[2,†]

[1]*Departamento de Fisica, Facultad de Ciencias Exactas y Naturales, Universidad de Buenos Aires–Ciudad Universitaria,*
1428 Buenos Aires, Argentina
[2]*Department of Physics, University of Maryland, College Park, Maryland 20742, USA*

We analyze the phenomena of condensate collapse, as described by Donley *et al.* [Nature **412**, 295 (2001)] and N. Claussen [Ph. D thesis, University of Colorado, 2003 (unpublished)] by focusing on the behavior of excitations or fluctuations above the condensate, as driven by the dynamics of the condensate, rather than the dynamics of the condensate alone or the kinetics of the atoms. The dynamics of the condensate squeezes and amplifies the quantum excitations, mixing the positive and negative frequency components of their wave functions thereby creating particles that appear as bursts and jets. By analyzing the changing amplitude and particle content of these excitations, our simple physical picture explains well the overall features of the collapse phenomena and provides excellent quantitative fits with experimental data on several aspects, such as the scaling behavior of the collapse time and the number of particles in the jet. The prediction of the bursts at this level of approximation is less than satisfactory but may be improved by including the backreaction of the excitations on the condensate. The mechanism behind the dominant effect—parametric amplification of vacuum fluctuations and freezing of modes outside of horizon—is similar to that of cosmological particle creation and structure formation in a rapid quench (which is fundamentally different from Hawking radiation in black holes). This shows that Bose-Einstein condensate dynamics is a promising venue for doing "laboratory cosmology."

I. INTRODUCTION

We introduce a perspective in the analysis of the phenomena of condensate collapse, described by Donley and co-workers [1,2], by focusing on the behavior of fluctuations above the condensate, rather than the condensate itself. We show that the condensate dynamics squeezes, amplifies, and mixes positive and negative frequency components of the wave functions of the condensate excitations. In addition to providing a good qualitative understanding of the general picture, our theory also produces precise predictions, specifically, on the critical number of particles at the first instance when the instability sets in, the scaling of the waiting time $t_{collapse}$, and the number of particles in a jet. In this rendition we point out the analogy between the evolution of quantum excitations of the collapsing condensate and the vacuum fluctuations parametrically amplified by the background space-time in the Early Universe, suggesting a new venue for "laboratory cosmology."

A condensate formed from a gas of cold (3 nK) rubidium atoms is rendered unstable by a sudden inversion of the sign of the interaction between atoms. After a waiting time $t_{collapse}$, the condensate implodes, and a fraction of the condensate atoms are seen to oscillate within the magnetic trap that contains the gas (see below and Ref. [1]). These atoms are said to belong to a "burst." In the experiments described by Donley and co-workers [1,2], the interaction is again suddenly turned off after a time τ_{evolve}. For a certain range of values of τ_{evolve}, new emissions of atoms from the conden-

sate are observed, the so-called "jets." Jets are distinct from bursts: they are colder, weaker, and have a distinctive disk-like shape.

The experiment of Donley and co-workers takes full advantage of the tunability of the effective atomic interaction due to a Feshbach resonance characteristic of ^{85}Rb [3,4]. The resonance is caused by the presence of a bound state whose binding energy may be tuned by means of an external magnetic field. In later experiments [5,6], observed fluctuations in the number of particles in the condensate have been well explained as arising from oscillations between the usual atomic condensate and a molecular state [7–12].

These oscillations were observed for magnetic fields in the order of 160 G, where the effective scattering length is of the order of $500a_0$ (and positive) ($a_0 = 0.529 \times 10^{-10}$ m is the Bohr radius) and the frequency of oscillations is of hundreds of kHz [5,6]. By contrast, in the experiment of Donley and co-workers [1] typical fields were around 167 G, the scattering length was only tens of Bohr radii (and negative) and the frequency of atom-molecule oscillations may be estimated as well over 10 MHz [13]. Under these conditions it is unlikely that the molecular condensate plays any important dynamical role, and indeed no oscillations are reported in the original paper (for the opposite view, see Ref. [14]). For these reasons and to highlight the mechanism particular to this experiment, we shall not include explicitly a molecular condensate in our model but discuss in detail the one-field model. However, if needed, this may be done in a very simple way, by including a second field to describe molecular destruction and creation operators [9,10,14]. We will elaborate on this point in a later subsection

There is a vast literature attempting to provide theoretical explanations of collapsing condensates [15–21]. In addition

*Email address: calzetta@df.uba.ar
†Email address: hub@physics.umd.edu

to speculations that collapse is due to molecular oscillations as alluded above (which we view as of secondary importance), the most serious theoretical attempt is based on the Gross-Pitaevskii (GP) equation with explicitly introduced nonlinear terms to account for multiparticle interactions [21,22]. We will show that the primary mechanism responsible for the main features of the experiment of Donley and co-workers [1,2] originates from the dynamics of quantum fluctuations around the background condensate field(s). We start with the Heisenberg operator for the many-body wave function and split it into a *c*-number part describing the condensate amplitude and a *q*-number part describing collective excitations (not individual atoms) above the condensate. We then derive an evolution equation for the wave-function operator of the quantum (noncondensate) excitations under an improved Hartree approach, the so-called Popov approximation [23–26].

In this paper, we use a "test field" approximation, by adopting (rather than deriving) the specific evolution of the condensate extracted from the experiment as given and study the dynamics of the excitations riding on this dynamics. Note that the experimentally given condensate dynamics is different from the mean-field dynamics obtained from a solution of the GP equation, because the former includes the dynamical effects of the fluctuations. Finding a self-consistent solution of the evolution equations for both the condensate and its fluctuations is called the "backreaction problem." It has been studied in detail in problems of similar contexts such as cosmological particle production (see below). Theoretical investigations for the Bose-Einstein condensate (BEC) fluctuations dynamics can be found in Refs. [7,27,28]. The squeezing of quantum unstable modes and its backreactions on the condensate have been considered before, e.g., as a damping mechanism for coherent condensate oscillations [29], and also applied to the description of condensate collapse [30–34]. Field-theory methods have recently been applied to the problem of formation and stability of Bose-Einstein condensates [35,36]. Fluctuations have also been considered by Góral *et al.* [37] and Graham and co-workers [38]. Our work differs from theirs in the emphasis we place on the behavior of the quantum excitations as a consequence of condensate dynamics.

Particularly relevant to the present work is Ref. [31], where condensate collapse is analyzed from the point of view that the physics is mainly due to the dynamics of quantum fluctuations, the same view as we hold here. There, the trapping potential is replaced by a normalizing box, whose volume is eventually taken to infinity. Our analysis in Secs. II and III is for a more realistic geometry, which enables us to compare quantitatively to experiments. The analysis of bursts versus jets given in Sec. IV however originates from a concept inspired by cosmological processes.

To the extent that many phenomena observed in connection to the collapse of this nature are essentially the result of a quantum fluctuation field (the noncondensate) interacting with a time-dependent background (the condensate), as we believe it is, there is a close analogy with similar processes in the Early Universe, specifically, vacuum particle creation from a time-dependent external field [39] or in a curved background space-time [40,41]. (For a squeezed state depiction of this process, see, e.g., Ref. [42], and references therein.) One could view condensate collapse as a laboratory realization of cosmological particle creation during quenching. (Note this is not the physical process behind black hole particle creation, as in the Hawking effect, much attention drawn to its detection in BEC notwithstanding [43].) In this process there is a competition between two (inverse) time scales, the physical frequency of the mode under consideration and the inverse collapse (expansion) rate of the condensate. In cosmology the inverse expansion rate is the Hubble constant for the background space time. While a mode whose physical frequency is higher than the Hubble constant, we refer to it as "inside the horizon," and its behavior is oscillatory. When the converse holds, the mode is "outside the horizon." They are depicted as "frozen" because they do not oscillate (see below), but are amplified [44]. This amplification is largely responsible for the observed primordial density contrast in the Universe [45].

In the condensate collapse problem, the role of the "Hubble" constant is played by the inverse growth (exponential) rate of the most unstable mode of the condensate, which is determined by the instantaneous number of particles in the condensate. Modes whose natural frequency is greater than the corresponding scale are relatively impervious to the dynamical condensate, but when the converse holds, consequences are drastic. When the exponential growth is the dominant factor, the mode is frozen; instead of oscillating, it is being amplified, a process that is analogous to the growth of fluctuations during spinodal decomposition [46].

In the same way that modes that left the horizon during inflation return during the radiation and matter dominated eras, giving rise to acoustic oscillations, as the unstable condensate sheds its atoms and approaches stability, the band of frozen modes narrows: we say that modes "thaw" as they turn from exponentially increasing to oscillatory behavior. The crux of the matter is that only oscillating modes are detected through destructive absorption imaging (see below). Whenever a mode thaws, it is perceived as if particles were being created. In the conditions of the experiment the initial number of actual particles above the condensate is negligible, and we may describe the phenomenon as particle creation from the vacuum.

To summarize, the key idea in our understanding of the phenomena associated with a condensate collapse is that of a dynamical background field of the condensate squeezing and mixing the positive and negative frequency components of its quantum excitations, thereby creating particles from the vacuum. The point of view of this work may be easily incorporated in a first-principles approach as taken in, e.g., Refs. [47–50]. The remarkable analogy between condensate collapse and quantum processes in the Early Universe and spinodal decomposition in phase transitions may stimulate new related experiments in BEC, to be carried out to address these problems in cosmology and condensed matter physics [51].

This paper is organized as follows. In Sec. II we briefly review the phenomenology of condensate collapse and set up the basic mathematical model. In Sec. III we give a discus-
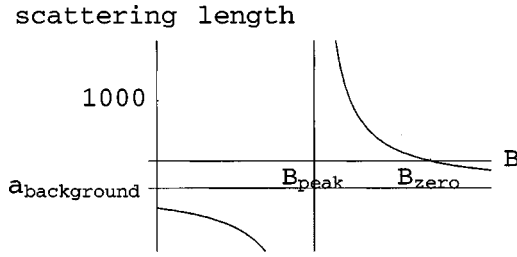
FIG. 1. (Color online) Effective scattering length as a function of applied magnetic field (unlike in the body of the paper, we follow here the usual sign convention). The scattering length is measured in multiples of Bohr radius $a_0 = 0.529 \times 10^{-10}$ m. The magnetic field is measured in Gauss. In the experiment by Donley and co-workers [1,2], the condensate is prepared at B_{zero} and then evolved to a *larger* field. In later experiments [5,6] the field was turned to a *lower* value, close to B_{peak} for a short time, and somewhere between B_{peak} and B_{zero} for the duration of the experiment.

sion of the onset of instability and of the scaling of the waiting time $t_{collapse}$ with the scattering length. In Sec. IV, we turn to a discussion of bursts and jets, based on the distinction between frozen and thawed modes. By postulating a specific condensate evolution (extracted from the experiment) we obtain quantitative predictions for the number of particles in a jet as a function of the time τ_{evolve} (when the scattering length is brought to zero). Our results are summarized in the final section. A few technical details are left to the appendixes.

II. THE MODEL

A. An overview of condensate collapse

In the Donley *et al.* experiment [1] a gas of N ^{85}Rb atoms at a temperature of 3 nK is prepared in a state where they behave essentially as a free gas within an anisotropic harmonic trap (see Figs. 1 and 2). The trap has a cylindrical geometry [let $\mathbf{r} \equiv (\rho, \varphi, z)$ be the usual cylindrical coordinates, with φ being the azimuthal angle]; the trap frequencies are $\nu_{radial} = 17.5$ Hz ($\omega_{radial} = 2\pi\nu_{radial} = 110$ Hz) and $\nu_{axial} = 6.8$ Hz ($\omega_{axial} = 42.7$ Hz). At time $t = 0$, the scattering length a (see below) is suddenly turned to a negative value $-a_{collapse}$. This configuration is known to be unstable whenever the number N_0 of atoms in the condensate exceeds $\kappa a_{ho}/|a|$, where a_{ho} is a characteristic length of the trap. The coefficient κ was reported as $\kappa = 0.46$ [52], but later measurements suggest it should be raised to $\kappa = 0.55$ [2,13].

For $N_0 = 6000$ atoms, the instability threshold is reported at $|a| = a_{cr} = 5.12 a_0$, where $a_0 = 0.529 \times 10^{-10}$ m. Therefore $a_{ho} = 5.6 \times 10^4 a_0 = 3 \times 10^{-6}$ m. If we write $a_{ho}^2 = \hbar/M\omega$ and introduce the atomic mass of $85 m_P \sim 1.3 \times 10^{-25}$ kg and $\hbar = 1.05 \times 10^{-34}$ Js, this corresponds to a frequency $\omega = 90$ Hz. This agrees well with the geometric average $\omega = (\omega_{axial}\omega_{radial}^2)^{1/3} = 80$ Hz. It follows that $t_{ho} = \omega^{-1} = 12.5$ ms.

In spite of the instability, over a time $t_{collapse}$ there is no significant decay of the condensate. $t_{collapse}$ depends very strongly on $a_{collapse}$ (see below). After $t_{collapse}$, the number of atoms in the condensate falls exponentially. If left to itself,
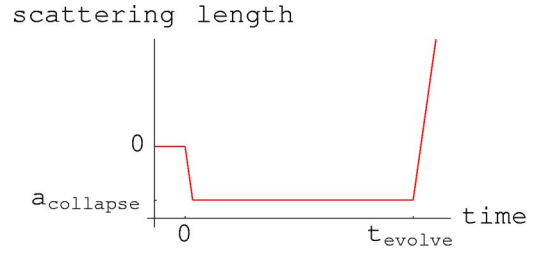

FIG. 2. (Color online) Qualitative evolution of the effective scattering length as a function of time in the experiment by Donley and co-workers [1,2] (unlike in the body of the paper, we follow here the usual sign convention). The scattering length in measured in multiples of Bohr radius $a_0 = 0.529 \times 10^{-10}$ m, time is measured in milliseconds. The condensate is prepared at $a = 0$, and then the effective interaction is made attractive. After a time τ_{evolve}, the interaction is made repulsive, which allows the condensate to expand and aids visualization.

the condensate eventually stabilizes retaining a number $N_{remnant}$ of atoms.

During this period, a cloud or burst of atoms is observed. These atoms oscillate in the radial direction with the trap radial frequency. The energy associated with the burst is larger in the radial direction than in the axial direction. The number of atoms in the burst increases with the time elapsed since the decay begins, with a time constant of about 1.2 ms; after 7 ms, the number of burst atoms stabilizes. About a fifth of the atoms in the condensate go into the burst, with variations of about 20%.

Condensate decay is interrupted at a time $t = \tau_{evolve}$, when the scattering length is again tuned to a positive value. If the condensate is already stabilized at τ_{evolve}, nothing too drastic happens, but otherwise a new phenomenon appears, namely the expulsion of a jet of atoms. Jets have much lower kinetic energy than bursts (a few nano-Kelvin).

B. Basic equations

The model[1] is based on the Hamiltonian operator for N interacting atoms with mass M in a trap

$$\hat{\mathbf{H}} = \int d\mathbf{r} \left\{ -\frac{\hbar^2}{2M}\mathbf{\Psi}^\dagger\nabla^2\mathbf{\Psi} + V(\mathbf{r})\mathbf{\Psi}^\dagger\mathbf{\Psi} - \frac{U}{2}\mathbf{\Psi}^{\dagger 2}\mathbf{\Psi}^2 \right\},$$
(1)

with the total number operator N given by

$$N = \int d\mathbf{r}\mathbf{\Psi}^\dagger\mathbf{\Psi}.$$
(2)

---

[1]In writing down the main equations of our model, we choose a sign convention that makes the effective coupling constant positive for an attractive interaction, and a system of units adapted to the problem. Taking the average frequency ω as reference, we may define length and time scales a_{ho} and t_{ho} (see above) and an energy scale $E_{ho} = \hbar\omega = M\omega^2 a_{ho}^2$. From now on, we shall choose units such that these three scales take value 1.

Here $\mathbf{V}(\mathbf{r})$ is the trap potential and U is (assumed to be a short ranged) the interaction between the atoms. We introduce a dimensionless field operator $\Psi(x)$,

$$\boldsymbol{\Psi}(r)\equiv a_{ho}^{-3/2}\Psi(x), \tag{3}$$

where a_{ho} is a characteristic length of the trap, and a dimensionless coupling constant u,

$$U\equiv\hbar\omega a_{ho}^3 u. \tag{4}$$

In terms of the scattering length a (which we define as positive for an attractive interaction), we have

$$U=\frac{4\pi\hbar^2 a}{M}. \tag{5}$$

So

$$u=\frac{4\pi\hbar a}{M\omega a_{ho}^3}=4\pi\left(\frac{a}{a_{ho}}\right). \tag{6}$$

The Hamiltonian and the trap potential can also be written in terms of dimensionless variables

$$\hat{H}=E_{ho}\hat{H}, \quad \mathbf{V}(\mathbf{r})=E_{ho}V(r). \tag{7}$$

Assuming a cylinder shaped potential

$$V(\mathbf{r})=\tfrac{1}{2}(\omega_z^2 z^2+\omega_\rho^2\rho^2), \tag{8}$$

with radial ρ and longitudinal z coordinates measured in units of a_{ho}, with associated (dimensionless) frequencies $\omega_z=\omega_{axial}/\omega\sim 1/2$ and $\omega_\rho=\omega_{radial}/\omega\sim\sqrt{2}$.

Ψ obeys the equation of motion

$$\dot{\Psi}=i[\hat{H},\Psi] \tag{9}$$

and the equal time commutation relations

$$[\Psi(t,\mathbf{r}),\Psi^\dagger(t,\mathbf{r}')]=\delta^{(3)}(\mathbf{r}-\mathbf{r}'), \tag{10}$$

whereby

$$i\frac{\partial\Psi}{\partial t}=H\Psi-u\Psi^\dagger\Psi^2. \tag{11}$$

Here

$$H=-\tfrac{1}{2}\boldsymbol{\nabla}^2+V(r) \tag{12}$$

is the (dimensionless) one-particle trap Hamiltonian. We decompose the Heisenberg operator Ψ into a c-number condensate amplitude Φ and a q-number noncondensate amplitude ψ, consisting of the fluctuations or excitations

$$\Psi(\mathbf{r},t)=\Phi(\mathbf{r},t)+\psi(\mathbf{r},t). \tag{13}$$

Then

$$\Psi^\dagger\Psi=|\Phi|^2+\Phi(\psi^\dagger+\psi)+\psi^\dagger\psi \tag{14}$$

and

$$n\equiv\langle\Psi^\dagger\Psi\rangle=|\Phi|^2+\langle\psi^\dagger\psi\rangle\equiv n_0+\tilde{n}, \tag{15}$$

where $\langle\rangle$ denotes the expectation value with respect to the initial quantum state. The cross terms vanish because the mean field is defined with zero fluctuations. Here $n_0=|\Phi|^2$ is the number density of the condensate and $\tilde{n}\equiv\langle\psi^\dagger\psi\rangle$ is the number density corresponding to the fluctuations. Further,

$$\Psi^\dagger\Psi^2=(\Phi*+\psi^\dagger)(\Phi^2+2\Phi\psi+\psi^2)$$
$$=|\Phi|^2\Phi+2|\Phi|^2\psi+\Phi^2\psi^\dagger+2\Phi\psi^\dagger\psi$$
$$+\Phi*\psi^2+\psi^\dagger\psi^2. \tag{16}$$

Under the self-consistent mean-field approximation [25]

$$\psi^\dagger\psi\simeq\langle\psi^\dagger\psi\rangle=\tilde{n}, \tag{17}$$

$$\psi^2\simeq\langle\psi^2\rangle=\tilde{m}, \tag{18}$$

where $\tilde{m}$ is sometimes called the anomalous density, and

$$\psi^\dagger\psi^2\simeq 0. \tag{19}$$

Taking the expectation value of the Heisenberg equation, we obtain the Gross-Pitaevskii equation (GPE)

$$i\frac{\partial\Phi}{\partial t}-H\Phi+u|\Phi|^2\Phi+u\{2\Phi\tilde{n}+\Phi*\tilde{m}\}=0. \tag{20}$$

Subtracting this from the original Eq. (10), and neglecting nonlinear terms, we obtain the equation for the fluctuation field

$$\left[i\frac{\partial}{\partial t}-H+2u|\Phi|^2\right]\psi(x)+u\Phi^2\psi^\dagger(x)=0. \tag{21}$$

This is the basic equation we shall use here for analyzing the behavior of the excitations (fluctuations) for a given condensate evolution. From the evolution of the fluctuations we can then calculate the modified evolution of the condensate. Note that only in taking the Bogoliubov approximation (setting $\tilde{n}=\tilde{m}=0$) will one get a closed equation, the Gross-Pitaevskii equation, for the condensate. In principle these two equations for fluctuations (21) and condensate (20) need be solved together in a self-consistent manner. (This is called the "backreaction problem" first studied in external field or cosmological particle creation problems.) Here we solve only the equation for the fluctuation field using the experimentally measured value for the background field. As mentioned earlier this is already a (lowest-order) backreaction-modified or self-consistent solution which is an improvement over the mean-field solution obtained from the GP equation.

We next parametrize the wave functions as

$$\Phi=\Phi_0 e^{-i\Theta}, \tag{22}$$

$$\psi=\psi_0 e^{-i\Theta}, \tag{23}$$

where Φ_0 and Θ are real. We seek to express the two equations for Φ, ψ by the three equations for the three real quantities Φ_0, ψ_0, Θ. Observe that

$$\nabla_x^2(Fe^{-i\Theta}) = e^{-i\Theta}\{\nabla_x^2 F - 2i\nabla\Theta\nabla F - [i\nabla^2\Theta + (\nabla\Theta)^2]F\},$$

(24)

therefore,

$$\frac{\partial\Theta}{\partial t} + \frac{1}{2}(\nabla\Theta)^2 - \frac{1}{\Phi_0}H\Phi_0 + u\Phi_0^2 + u\{2\tilde{n} + \text{Re }\tilde{m}\} = 0,$$

(25)

$$\frac{\partial\Phi_0}{\partial t} + \nabla\Theta\nabla\Phi_0 + \frac{1}{2}(\nabla^2\Theta)\Phi_0 + u\Phi_0\text{Im }\tilde{m} = 0, \quad (26)$$

$$\left[i\frac{\partial}{\partial t} - H + 2u\Phi_0^2\right]\psi_0 + u\Phi_0^2\psi_0^\dagger + \psi_0\frac{\partial\Theta}{\partial t} + i\nabla\Theta\nabla\psi_0$$

$$+ \frac{1}{2}[i\nabla^2\Theta + (\nabla\Theta)^2]\psi_0 = 0.$$

(27)

The third equation may be simplified by using the first equation,

$$\left[i\left(\frac{\partial}{\partial t} + (\nabla\Theta)\nabla + \frac{1}{2}\nabla^2\Theta\right) - H + \frac{1}{\Phi_0}(H\Phi_0) + u\Phi_0^2\right]\psi_0$$

$$+ u\Phi_0^2\psi_0^\dagger = 0.$$

(28)

We have also neglected terms which were nonlinear in fluctuations.

III. ONSET OF COLLAPSE AND SCALING OF $t_{collapse}$

A. The early stage

During the first few milliseconds of evolution, we may regard the condensate density as time independent, and the condensate phase as homogeneous (see Appendix A for justification). We may then write the equation for the fluctuation field Eq. (21) as

$$\left[i\frac{\partial}{\partial t} - H + E_0\right]\psi_0 + u\Phi_0^2(\psi_0 + \psi_0^\dagger) = 0,$$

(29)

$$E_0 = \frac{1}{2}(\omega_z + 2\omega_\rho).$$

(30)

To solve this equation we decompose it into a self-adjoint and an antiadjoint part

$$\psi_0 = \xi + i\eta,$$

(31)

with each part satisfying an equation:

$$\frac{\partial\xi}{\partial t} = [H - E_0]\eta,$$

(32)

$$\frac{\partial\eta}{\partial t} + [H - E_0 - 2u\Phi_0^2]\xi = 0.$$

(33)

In the subspace orthogonal to the condensate, the operator has an inverse, hence

$$\eta = [H - E_0]^{-1}\frac{\partial\xi}{\partial t},$$

(34)

and since the trap Hamiltonian is time independent, we have

$$\frac{\partial^2\xi}{\partial t^2} + [H - E_0]H_{eff}\xi = 0.$$

(35)

Here

$$H_{eff} = H - E_0 - 2u\Phi_0^2$$

(36)

is the Hamiltonian for a particle moving in the potential

$$V(r) = \frac{1}{2}[\omega_z^2 z^2 + \omega_\rho^2\rho^2 - Ae^{-r^2} - 2E_0],$$

(37)

where $r^2 = \omega_z z^2 + \omega_\rho\rho^2$ and $A = 4N_0 u/\pi^{3/2}$. [Recall from experiment that the condensate is stable for $A \leq 16(0.55)/\sqrt{\pi} = 4.96$].

Suppose $[H - E_0]H_{eff}$ has eigenvectors ψ_K, with eigenvalues λ_K, we can expand

$$\xi = \sum_n c_K(t)\psi_K.$$

(38)

Then $c_K(t)$ will be a superposition of two harmonic oscillations with frequencies $\pm\sqrt{\lambda_K}$. To have an unstable condensate it is necessary that at least one of the λ_K is negative; the boundary of stability occurs when the lowest λ_K, say λ_0, is exactly zero. Since $[H - E_0]$ has an inverse, the equation $[H - E_0]H_{eff}\psi_0 = 0$ implies $H_{eff}\psi_0 = 0$.

In conclusion, the onset of collapse corresponds to the minimum value of the condensate density for which the effective Hamiltonian H_{eff} develops a zero mode.

B. The onset of collapse

We shall now study the spectrum of the operator H_{eff}. The idea is that the low-lying states, which are the most relevant ones to our discussion, will try to keep close to where the potential is a minimum, namely, the origin. If the width of the state is small enough, the potential will be nearly harmonic.

One further consideration is that we are interested in the part of the fluctuation field which remains orthogonal to the condensate, since fluctuations along the condensate mode may be interpreted as condensate fluctuations rather than particle loss. This is granted for all modes with odd parity; for modes of even parity, it means that a certain combination must be excluded. The ground state of H_{eff} is certainly not orthogonal to the condensate, since neither has nodes.

A simple but remarkably accurate way of determining whether or not H_{eff} admits a zero mode is to consider its expectation value $\langle H_{eff}\rangle$ with respect to some appropriate trial state. The first excited eigenvalue E_{100} is the minimum possible expectation value, taken with respect to any normalized state orthogonal to the ground state. Therefore, if we

may exhibit a wave function leading to a negative $\langle H_{eff} \rangle$, then necessarily E_{100} is negative as well.

Let us write

$$H_{eff} = H_0^z + H_0^\rho - 2u\Phi_0^2 - E_0, \tag{39}$$

$$H_0^z = \frac{p_z^2}{2} + \frac{\omega_z^2 z^2}{2}, \tag{40}$$

$$H_0^\rho = \frac{p_\rho^2}{2} + \frac{\omega_\rho^2 \rho^2}{2}. \tag{41}$$

Recall for the condensate

$$\Phi_0^2 = \frac{N_0}{\pi^{3/2}} e^{-[\omega_z z^2 + \omega_\rho \rho^2]}. \tag{42}$$

We shall try to minimize the expectation value of H with respect to a wave function of the form

$$\psi_1^{\Omega_z}(z) \psi_0^{\Omega_\rho}(x) \psi_0^{\Omega_\rho}(y), \tag{43}$$

where ψ_0^Ω and ψ_1^Ω are the fundamental and first excited states of a one-dimensional harmonic oscillator with arbitrary frequency Ω,

$$\psi_0^\Omega = \left(\frac{\Omega}{\pi}\right)^{1/4} e^{-\Omega z^2/2}, \tag{44}$$

$$\psi_1^\Omega = \left(\frac{4\Omega}{\pi}\right)^{1/4} (\Omega^{1/2} z) e^{-\Omega z^2/2}. \tag{45}$$

The free part yields

$$\langle H_0^z \rangle = \frac{3}{4}\left(\Omega_z + \frac{\omega_z^2}{\Omega_z}\right), \tag{46}$$

$$\langle H_0^\rho \rangle = \frac{1}{2}\left(\Omega_\rho + \frac{\omega_\rho^2}{\Omega_\rho}\right). \tag{47}$$

The condensate part yields

$$\int d^3 r \Phi_0^2(r) [\psi_1^{\Omega_z}(z) \psi_0^{\Omega_\rho}(x) \psi_0^{\Omega_\rho}(y)]^2$$

$$= \frac{N_0}{\pi^{3/2}} \Omega_\rho \Omega_z^{3/2} (\omega_z + \Omega_z)^{-3/2} (\omega_\rho + \Omega_\rho)^{-1}. \tag{48}$$

Putting them together

$$\langle H_{eff} \rangle = \frac{1}{2}\left[\frac{3}{2}\left(\Omega_z + \frac{\omega_z^2}{\Omega_z}\right) + \left(\Omega_\rho + \frac{\omega_\rho^2}{\Omega_\rho}\right) - \omega_z - 2\omega_\rho \right.$$

$$\left. - \frac{A}{\left(1 + \frac{\omega_z}{\Omega_z}\right)^{3/2} \left(1 + \frac{\omega_\rho}{\Omega_\rho}\right)} \right], \tag{49}$$

where

$$A = 4u \frac{N_0}{\pi^{3/2}} = \frac{16}{\sqrt{\pi}}\left(N_0 \frac{a}{a_{ho}}\right). \tag{50}$$

If we adopt the values $\omega_z = 1/2$, $\omega_\rho = \sqrt{2}$, relevant to the JILA experiment, then we obtain $\langle H_{eff} \rangle = 0$ for the first time when $A = A_{crit} \sim 4.6$, $\Omega_z \sim 0.78$, and $\Omega_\rho \sim 1.7$. From the definition of A, we conclude that instability will occur when

$$N_0 \frac{a_{crit}}{a_{ho}} = \kappa = \frac{\sqrt{\pi}}{16} A_{crit} = 0.51. \tag{51}$$

This result compares remarkably well with the experimental value $\kappa = 0.55$, as well as with the theoretical estimate presented in Ref. [53]. This agreement may be seen as natural, as the equations we postulate for the fluctuations may be obtained from the linearization of the GPE, discarding both $\tilde{n}$ and $\tilde{m}$. In both calculations, the geometry of the trap plays a fundamental role.

C. Scaling of $t_{collapse}$

As we have already noted, even for condensate densities above the stability limit, no particle is seen to be lost from the condensate during a waiting time $t_{collapse}$.

Even in the absence of a detailed model of the condensate evolution, the above analysis allows us to make a definite prediction of the way $t_{collapse}$ scales with the scattering length. The basic idea is that, while $t_{collapse}$ depends in a complex way on several time scales, some intrinsic to the condensate and some related to the condensate-noncondensate interaction, up to $t_{collapse}$ the time scales intrinsic to the condensate are very large compared to the other processes. The nontrivial point is that even in this limit the time scales of the noncondensate remain finite, and so they fix the scale for $t_{collapse}$ itself. Using the exponential growth of the first excited state as a measure, we are led to the estimate $t_{collapse} \sim \varepsilon^{-1}$.

Consider a value of A close to, yet higher than, the critical one. The fastest growing mode is the eigenvector of $[H - E_0]H_{eff}$ with most negative eigenvalue, say $-\sigma$. When A takes the critical value A_{cr}, $\sigma = 0$. Close to the critical point, we may compute σ using time independent perturbation theory, even if $[H - E_0]H_{eff}$ is not Hermitian. The idea is that at the critical value of A there is a single normalized state $|100\rangle$ orthogonal to the condensate such that $[H - E_0]H_{eff}|100\rangle = 0$ and

$$\langle 100|[H - E_0]H_{eff}|\psi\rangle + \langle\psi|[H - E_0]H_{eff}|100\rangle = 0 \tag{52}$$

for any state $|\psi\rangle$ orthogonal to both condensate and $|100\rangle$ (otherwise, there would be states orthogonal to the condensate with $\langle[H - E_0]H_{eff}\rangle < 0$, which is impossible). Now for A slightly above the critical value, let $|\sigma\rangle = |100\rangle + |\delta\sigma\rangle$, $\langle 100|\delta\sigma\rangle = 0$ be the eigenstate corresponding to the minimum eigenvalue $-\sigma$. Then

$$-\sigma = \langle 100 | [H - E_0] H_{eff} | \sigma \rangle$$

$$= \langle 100 | [H - E_0] H_{eff} | 100 \rangle + \text{higher-order terms}$$

$$(53)$$

and so

$$\sigma \sim \left(\frac{A}{A_{crit}} - 1 \right) \langle [H - E_0] 2 u \Phi_0^2 \rangle, \qquad (54)$$

where the expectation value is computed at the critical point. Since we know the form of the wave function, computing the expectation value is a simple exercise. We find that the growing mode increases as $\exp \varepsilon t$, where

$$\varepsilon = \sqrt{\sigma} \sim T \left(\frac{A}{A_{crit}} - 1 \right)^{1/2} \qquad (55)$$

and $T = \langle [H - E_0] 2 u \Phi_0^2 \rangle \sim 0.6$. Since $A/A_{crit} = a/a_{cr}$ for the given total number of atoms,

$$t_{collapse} = t_{crit} \left(\frac{a}{a_{cr}} - 1 \right)^{-1/2}. \qquad (56)$$

The power-law Eq. (56) describes with great accuracy the way $t_{collapse}$ scales with the scattering length; the actual prediction $t_{crit} \sim T^{-1}$ is correct only as an order of magnitude estimate. In natural units, T^{-1} is about 20 ms, while the best fit to the experimental data is obtained for $t_{crit} \sim 5$ ms.

We should stress that the factor of 4 discrepancy between our prediction and the experimental result could be easily explained away in terms of a more complete model of condensate depletion. For example, the probability for two particles in the condensate to collide and transfer to the growing mode, Bose enhanced by the population in the latter, would go as $(\psi^\dagger \psi)^2$, thereby yielding the factor of 4 in the exponent. However, in this paper we shall keep to our goal of providing the simplest theory which gives the best qualitative description of the condensate collapse phenomena, hereby understood as arising from the quantum dynamics of the fluctuations.

An analysis of collapse based on the Popov approximation equations, for a simplified geometry, is given in Ref. [31]. However, the time $t_{NL} \sim (u N_0)^{-1}$ [54], which is herewith identified as characteristic of collapse, does not account for the enhancement of $t_{collapse}$ near the critical point.

In Fig. 3 we plot the scaling law (56) (full line) derived here and compare it with the experimental data for $N_0 = 6000$ as reported in Refs. [1,2] (small black points), the $t_{NL} \sim (u N_0)^{-1}$ prediction (suitable scaled) as given in Refs. [31,2] (dashed line) and the results of numerical simulations reported in Ref. [21] (large gray dots). While all three theoretical predictions may be considered satisfactory, the $t_{NL} \sim (u N_0)^{-1}$ fails to describe the divergence of $t_{collapse}$ as the critical point is approached. The results of numerical simulations reported in Ref. [21] based on an improved Gross-Pitaevskii equation tend to be systematically above the experimental results. In a classical instability, the unstable modes must grow from zero, while in a quantum instability,
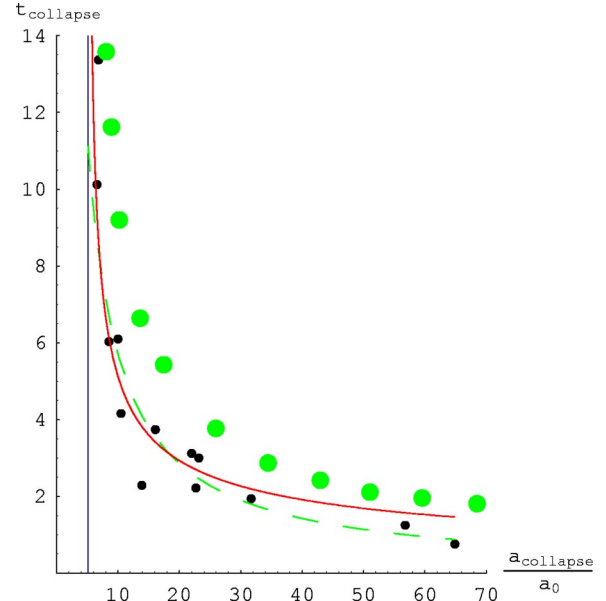

FIG. 3. (Color online) Plot of $t_{collapse}$ (in milliseconds) against $a_{collapse}$ (in multiples of Bohr radius $a_0 = 0.529 \times 10^{-10}$ m). We plot the scaling law Eq. (56) (full line) and compare it against the experimental data for $N_0 = 6000$ as reported in Refs. [1,2] (small black dots), the $t_{NL} \sim (u N_0)^{-1}$ prediction (suitably scaled) as given in Refs. [31,2] (dashed line), and the results of numerical simulations reported in Ref. [21] (large gray dots). While all three theoretical predictions may be considered satisfactory, the $t_{NL} \sim (u N_0)^{-1}$ fails to describe the divergence of $t_{collapse}$ as the critical point is approached. The results of numerical simulations based on an improved Gross-Pitaevskii equation tend to be systematically above the experimental results. In a classical instability, the unstable modes must grow from zero, while in a quantum instability, they are always seeded by their own zero-point fluctuations, which speeds up the development of the instability. Therefore, the fact that numerical simulations tend to overestimate $t_{collapse}$ may be a further indication of the quantum origin of the phenomenon.

they are always seeded by their own zero-point fluctuations, which speeds up the development of the instability. Therefore, the fact that numerical simulations based on classical instability tend to overestimate $t_{collapse}$ may be a further indication of the quantum origin of the phenomenon.

D. Minor role of a molecular condensate

Having obtained some insight into the early stages of collapse, let us discuss briefly how the present model may be modified to explicitly account for the population of a molecular state. We refer the reader to Refs. [10,14,11] for further details.

The system of atoms and molecules at the Feshbach resonant state may be described by a theory where the fundamental degrees of freedom are an atomic field $\Psi(x)$ (we use the dimensionless amplitude introduced in the preceding Section) and a molecular field $A(x)$. The Hamiltonian takes the form

$$H = H_{atom} + H_{mol} + H_{be} + H_{int}, \qquad (57)$$

where

$$H_{atom} = H_{trap} + H_{bkgd}. \tag{58}$$

Here H_{trap} given in Eq. (12) describes the dynamics of free atoms in the trap, H_{bkgd} accounts for the background interaction between atoms (that is, very far from resonance)

$$H_{bkgd} = \left(\frac{-u_{bkgd}}{2} \right) \int d^3x \Psi^{\dagger 2} \Psi^2(x), \tag{59}$$

where [6] (recall that our sign convention is a positive scattering length for an attractive interaction)

$$u_{bkgd} = 4\pi \frac{a_{bkgd}}{a_{ho}}, \quad a_{bkgd} = 450 a_0 \Rightarrow u_{bkgd} = 0.1. \tag{60}$$

H_{mol} describes the motion of molecules in the trap. We treat a molecule as a particle of mass $2M$ (where M is the mass of the atom) subject to a potential $2V$ (where V is the trap potential seen by the atoms) [55], so the frequency of oscillations in the trap is the same for atoms and molecules. H_{be} accounts for the energy difference between a molecule and two atoms

$$H_{be} = -\varepsilon(B) \int d^3x A^{\dagger} A(x). \tag{61}$$

Plots of the binding energy $\varepsilon(B)$ as a function of the applied field B are given in Refs. [8,13]. Finally, H_{int} accounts for the formation and dissociation of molecules:

$$H_{int} = \Gamma \int d^3x (A^{\dagger} \Psi^2 + \Psi^{\dagger 2} A)(x). \tag{62}$$

The binding energy $\varepsilon(B)$ is the crucial input parameter in the model. $\varepsilon(B) = 0$ at the resonance field $B = B_{peak} = 155$ G [13] and increases with larger B's. At values of $B \sim 156$ G typical of the Ramsey fringes experiment [6] we already have binding energies of the order of 10 KHz; this is much larger than 100 Hz typical of motion in the trap, and therefore H_{mol} is negligible (in the condensate collapse experiment [1] typical fields where $B \sim 167$ G, and $\varepsilon(B)$ was much larger). Under this approximation, the *full* Heisenberg equation of motion for the molecular field

$$i \frac{\partial}{\partial t} A = -\varepsilon(B) A + \Gamma \Psi^2 \tag{63}$$

may be solved analytically

$$A(r,t) = A(r,0) e^{i\varepsilon t} - i\Gamma \int_0^t dt' e^{i\varepsilon(t-t')} \Psi^2(r,t'). \tag{64}$$

If the atomic field is slowly varying in the scale of ε^{-1}, then the integral is dominated by the upper limit, and simplifies to

$$A(r,t) = A_{free}(r,t) + \frac{\Gamma}{\varepsilon} \Psi^2(r,t). \tag{65}$$

The free part decouples from the atomic condensate, and the effect of the driven part is to introduce an effective interaction among atoms, so that u_{bkgd} in H_{bkgd} is replaced by

$$u_{eff} = u_{bkgd} - \frac{2\Gamma^2}{\varepsilon(B)}, \tag{66}$$

which is the familiar pattern that makes it possible to tune the scattering length. The effective scattering length vanishes at $B = B_{zero} = 165.75$ G [13] (see Fig. 1).

We conclude that under this approximation, the number of molecules—disregarding those already present independently of the atomic condensate—is

$$N_{mol} \sim \left(\frac{\Gamma}{\varepsilon} \right)^2 N_{atom}^2 = \frac{u_{bkgd}}{2\varepsilon(B)} \left(1 - \frac{u_{eff}}{u_{bkgd}} \right) N_{atom}^2. \tag{67}$$

If $N_{atom} \sim 16\,000$ and $u_{eff} \sim -u_{bkgd}$ [6], then the molecular condensate becomes important when $\varepsilon(B) \sim u_{bkgd} N_{atom} \omega_{ho} = 128$ kHz. This regime was achieved in Ref. [6]. Under these conditions we cannot rely on the above approximation, but rather we must solve the model. This yields atom-molecule oscillations with a frequency set by $\varepsilon(B)$.

In contrast, in the condensate collapse experiment [1] the magnetic field was driven *above* B_{zero}, with typical values $B = 167$ G. For these fields, the molecular binding energy is close to 12 MHz (see Refs. [13,56]), or $15 \times 10^4 \omega_0$ Therefore $N_{mol} \sim 0.005 N_{atom} \sim 80$. This is less than the number of atoms even in the earliest measured jets (see Ref. [1] and below), suggesting that no major role is played by molecular recombination. This conclusion is consistent with the fact that no oscillations in the number of particles in the condensate are seen (see [1] and below). It is interesting to observe that the numerical simulations presented in Ref. [14] assume a set of parameters chosen to display the effect most clearly, not attempting to be realistic.

This leaves open the possibility that the approximation may break down because the atomic field is not slowly varying with respect to ε^{-1}. For example, the time it takes to change the magnetic field from B_{zero} to B_{evolve} is probably of the order of 10 μs$= 8 \times 10^{-4} \omega_{ho}^{-1}$ [6]. This is a short time compared to ε^{-1} under the conditions of the Ramsey fringes experiment [6], but a rather easy stroll in the condensate collapse experiment [1]. The next scale in which we expect the condensate to react (which is also of the order of the inverse atomic chemical potential) is t_{NL} [54,31], but this is of the order of milliseconds and therefore way too long.

The conclusion is that formation or dissociation of molecules, under the conditions of the condensate collapse experiment [1], is unlikely to have played a central role. Moreover, in models where the molecular state is explicitly included, it is still necessary to account for the quantum dynamics of the atomic field. This is done, for example, in Ref. [14] by tracking the fluctuation two-point functions along with the condensates, or in Ref. [11] by providing independent equations for the anomalous atom pair amplitude. Resonance of molecular field with the condensate alone, though remarkably successful in the later experiments, cannot account for the phenomena of this experiment. For the experi-

ment of Donley and co-workers [1,2] the dominant qualitative features are determined by the dynamical vacuum squeezing mechanism proposed here; including a molecular field can only provide a minor quantitative improvement.

IV. EVOLUTION OF FLUCTUATIONS: BURSTS AND JETS

In the preceding section, we were mostly concerned with identifying the factors that can render the condensate unstable. In this section, we shall consider the quantum evolution of fluctuations, as a test field riding on the collapsing condensate extracted from experiment. The basic dynamical equations are, from before, Eqs. (31)–(33), where now Φ_0^2 is assumed to have both space and time dependence. The initial state is defined by the condition that $u=0$ for $t<0$; we shall take it to be the particle vacuum $|0\rangle$, which is defined by $\psi(x,0)|0\rangle=0$ everywhere. Rather than seeking a rigorous solution, we wish to understand the structure of the problem in order to display the extent to which the phenomenology of condensate collapse is determined by fundamental (yet simple) quantum dynamical effects such as parametric amplification and particle creation. With this goal in mind, we shall make some physically motivated simplifications.

We have already seen that it is possible to introduce a mode decomposition of the ξ operator based on the eigenfunctions of $[H-E_0]H_{eff}$. This shows that the preconceived notion that fluctuations will react only to the local state of the condensate is flawed; the relevant modes are nonlocal and can sample conditions over a large portion of the trap.

For short wavelengths λ, we expect these eigenfunctions will approach trap eigenmodes, since $H\sim\lambda^{-2}\gg 2u\Phi_0^2$. Also the fact that particles in bursts are seen to oscillate with the trap frequencies [1] suggests that their dynamics is determined by the trap Hamiltonian (see below). Of course, the trap eigenmodes would also be eigenfunctions of H_{eff} if this operator and H commuted. Now, since

$$[H,H_{eff}]=u\{\nabla^2\Phi_0^2+2\nabla\Phi_0^2\nabla\}, \tag{68}$$

we see that we may disregard the commutator when the condensate is slowly varying with respect to the relevant modes. Early enough in the collapse, the typical scale for the condensate is a_{ho}, and this condition will hold for almost every mode. Thus we shall make the approximation of assuming a homogeneous condensate. The amplitude of the homogeneous condensate will be chosen to enforce the onset of instability. Since we expect the lowest trap mode to become unstable when $N=N_{cr}=\kappa/a$ (in units where $a_{ho}=1$), we approximate

$$2u\Phi_0^2\equiv\left(\frac{a}{\kappa}\right)\omega_z N_0(t), \tag{69}$$

where $N_0(t)$ is the instantaneous total number of particles in the condensate. For constant N_0, this yields $\varepsilon\sim\omega_z(a/a_{cr}-1)^{1/2}$ for the time constant of the growing mode, which is close to the more rigorous estimate Eq. (55), above.

In practice, κ^{-1} in Eq. (69) is a measure of the overlap between the condensate and the excitation modes, as in Eq.
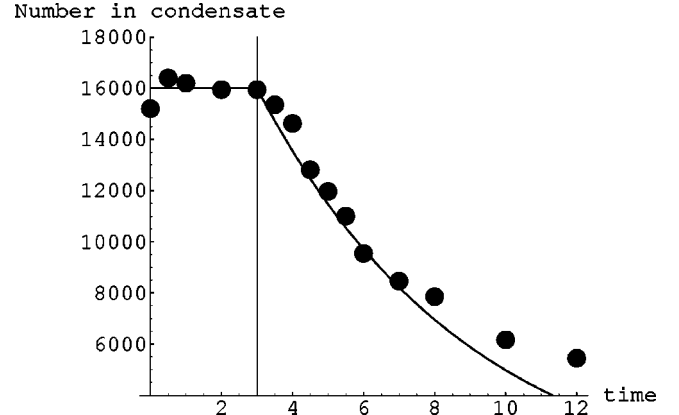

FIG. 4. The evolution for the number of particles in the condensate $N(t)$ as a function of time (measured in milliseconds) assumed for the calculation of the number of particles in a jet. For comparison, we have superimposed the data from Fig. 1(b) of Ref. [1]. The agreement is satisfactory for our purposes, as we shall not consider the evolution beyond $\tau_{evolve}=12$ ms nor the formation of a remnant.

(48) above. Therefore, the approximation may be improved by adjusting κ according to the range of modes where it will be applied. We shall adopt this practice in what follows.

A. Evolution of fluctuations up to $t_{collapse}$

We now proceed with the quantitative analysis of condensate collapse. We assume a given evolution extracted from experiment for the number of particles in the condensate and analyze the evolution of fluctuations treated as a test field on this dynamic background.

Concretely, we shall consider evolutions where the number of particles in the condensate remains constant from the time $t=0$ when the scattering length is switched to a negative value up to some time $t_{collapse}$, and decays exponentially from then on (see Fig. 4). In the actual experiments the condensate does not evaporate completely, but the number of particles in the remnant is much smaller than the initial number of atoms in the condensate, and is therefore negligible at the early times when the approximation of a homogeneous condensate is valid.

Let us begin by considering the evolution up to the time of collapse $t_{collapse}$, or the waiting period. Let $\bar{N}_0$ be the initial number of particles in the condensate, and $a_{cr}=\kappa/\bar{N}_0$ be the corresponding critical scattering length. Trap eigenfunctions are labeled by a string of quantum numbers $\vec{n}=(n_z,n_x,n_y)$. The eigenvalues of the trap Hamiltonian are (with the zero energy already subtracted) $E_{\vec{n}}=\vec{n}\cdot\vec{\omega}$ where $\vec{\omega}=(\omega_z,\omega_\rho,\omega_\rho)$ and $\vec{n}\cdot\vec{\omega}=\omega_z n_z+\omega_\rho(n_x+n_y)$. We choose the eigenfunctions $\psi_{\vec{n}}$ to be real.

Let us expand

$$\psi=\sum_{\vec{n}}a_{\vec{n}}(t)\psi_{\vec{n}}(r), \tag{70}$$

$$\xi = \sum_{\vec{n}} c_{\vec{n}}(t) \psi_{\vec{n}}, \tag{71}$$

$$\eta = \sum_{\vec{n}} b_{\vec{n}}(t) \psi_{\vec{n}}. \tag{72}$$

Then

$$c_{\vec{n}} = \tfrac{1}{2}(a_{\vec{n}} + a_{\vec{n}}^{\dagger}), \tag{73}$$

$$b_{\vec{n}} = \frac{1}{2i}(a_{\vec{n}} - a_{\vec{n}}^{\dagger}), \tag{74}$$

$$\frac{d}{dt} b_{\vec{n}} = -\left[E_{\vec{n}} - \left(\frac{a}{a_{cr}}\right)\omega_z\right]c_{\vec{n}}, \tag{75}$$

$$\frac{d}{dt} c_{\vec{n}} = E_{\vec{n}} b_{\vec{n}}. \tag{76}$$

We see that there are two kinds of modes, stable (oscillatory, or thawed) modes if $E_{\vec{n}} > (a/a_{cr})\omega_z$, and unstable (growing, or frozen) modes if not. We shall consider each kind in turn.

B. Stable modes and bursts

First consider the case when $E_{\vec{n}} > (a/a_{cr})\omega_z$. We get

$$c_{\vec{n}}(t) = \frac{1}{2}(a_{\vec{n}} + a_{\vec{n}}^{\dagger})(0)\cos \omega_{\vec{n}} t + \frac{1}{2i\chi_{\vec{n}}}(a_{\vec{n}} - a_{\vec{n}}^{\dagger})(0)\sin \omega_{\vec{n}} t, \tag{77}$$

$$b_{\vec{n}}(t) = \frac{1}{2i}(a_{\vec{n}} - a_{\vec{n}}^{\dagger})(0)\cos\omega_{\vec{n}} t - \frac{1}{2}\chi_{\vec{n}}(a_{\vec{n}} + a_{\vec{n}}^{\dagger})(0)\sin \omega_{\vec{n}} t, \tag{78}$$

where

$$\omega_{\vec{n}} = \sqrt{E_{\vec{n}}\left[E_{\vec{n}} - \left(\frac{a}{a_{cr}}\right)\omega_z\right]} = \chi_{\vec{n}} E_{\vec{n}}, \tag{79}$$

$$\chi_{\vec{n}} = \sqrt{1 - \left(\frac{a}{a_{cr}}\right)\frac{\omega_z}{E_{\vec{n}}}}. \tag{80}$$

So

$$a_{\vec{n}}(t) = f_{\vec{n}}(t) a_{\vec{n}}(0) + g_{\vec{n}}(t) a_{\vec{n}}^{\dagger}(0), \tag{81}$$

where

$$f_{\vec{n}}(t) = \cos \omega_{\vec{n}} t + \left[2 - \left(\frac{a}{a_{cr}}\right)\frac{\omega_z}{E_{\vec{n}}}\right]\frac{\sin \omega_{\vec{n}} t}{2i\chi_{\vec{n}}}, \tag{82}$$

$$g_{\vec{n}}(t) = -\left(\frac{a}{a_{cr}}\right)\frac{\omega_z}{E_{\vec{n}}}\frac{\sin \omega_{\vec{n}} t}{2i\chi_{\vec{n}}}. \tag{83}$$

Observe that

$$|f_{\vec{n}}(t)|^2 - |g_{\vec{n}}(t)|^2 = \cos^2\omega_{\vec{n}} t + \left\{\left[2 - \left(\frac{a}{a_{cr}}\right)\frac{\omega_z}{E_{\vec{n}}}\right]^2 - \left(\frac{a}{a_{cr}}\frac{\omega_z}{E_{\vec{n}}}\right)^2\right\}\frac{\sin^2\omega_{\vec{n}} t}{4\chi_{\vec{n}}^2} = 1, \tag{84}$$

as required by the commutation relations. Although we assume vacuum initial conditions, these modes do not remain empty. The density

$$\tilde{n}(r,t) = \sum_{\vec{n}} \psi_{\vec{n}}^2(r)\langle a_{\vec{n}}^{\dagger}(t) a_{\vec{n}}(t)\rangle = \sum_{\vec{n}} \psi_{\vec{n}}^2(r)|g_{\vec{n}}(t)|^2$$

$$= \frac{1}{8}\left(\frac{a}{a_{cr}}\right)^2\omega_z^2 \sum_{\vec{n}} \psi_{\vec{n}}^2(r)\frac{\sin^2\omega_{\vec{n}} t}{\omega_{\vec{n}}^2}. \tag{85}$$

We see that the density has a constant term and an oscillatory term. In our view this oscillatory term is responsible for the appearance of bursts of particles oscillating within the trap. This point is worth some elaboration, as it will make clearer the contrast with the unstable modes to be discussed below.

Let us approximate the amplitudes $\psi_{\vec{n}}(r)$ by their WKB forms

$$\psi_{\vec{n}}(r) = \prod_{i=1-3} \psi_i(r_i), \tag{86}$$

$$\psi_i(r_i) = \frac{1}{\sqrt{p_i}}\cos\left[S_i - n_i\frac{\pi}{2}\right], \tag{87}$$

where

$$S_i = \int_0^{r_i} dx\, p_i(x), \tag{88}$$

$$p_i = \sqrt{2n_i\omega_i - \omega_i^2 r_i^2}. \tag{89}$$

After expanding all trigonometric functions, we see that the oscillatory part is a linear combination of terms of the form

$$\exp\left\{2i\left[\sum S_i - \omega_{\vec{n}} t\right]\right\} \tag{90}$$

in all sign combinations. If we look at the density at a given point and time (r,t), we see that the modes that contribute effectively are those for that (in the limit $\chi_{\vec{n}} \to 1$, $E_{\vec{n}} \gg \omega_z$)

$$\omega_i\left[\int_0^{r_i} \frac{dx}{p_i(x)} - t\right] = 0. \tag{91}$$

This equation describes a particle that moves along a classical trajectory in the trap potential, starting from the origin at $t=0$ with momentum $p_i(0)$. If we include the phase shift in computing the saddle point, there is a time delay, but it is the same for all particles.

We conclude that the oscillatory part of the density describes a swarm of particles moving along classical trajecto-

ries in the trap potential. These trajectories return to the origin at multiples of the inverse trap frequencies, thus producing a surge in the local density, which becomes large enough to be seen by destructive absorption imaging. These particles constitute the so-called bursts observed in the experiment of Donley and co-workers [1,2].

C. Unstable modes and jets

Let us now consider the opposite case $E_n^- \lesssim (a/a_{cr}) \omega_z$. Formally we may obtain the relevant formulas from the last section with the replacement $\chi_n^- = i \vartheta_n^-$, $\omega_n^- = i \sigma_n^-$, thus transforming $\cos \omega_n^- t \rightarrow \cosh \sigma_n^- t$ and $\sin \omega_n^- t \rightarrow i \sinh \sigma_n^- t$. We get

$$c_n^-(t) = \frac{1}{2}(a_n^- + a_n^{-\dagger})(0)\cosh\sigma_n^- t + \frac{1}{2i\vartheta_n^-}(a_n^- - a_n^{-\dagger})(0)\sinh\sigma_n^- t,$$

(92)

$$b_n^-(t) = \frac{1}{2i}(a_n^- - a_n^{-\dagger})(0)\cosh\sigma_n^- t$$

$$+ \frac{1}{2}\vartheta_n^-(a_n^- + a_n^{-\dagger})(0)\sinh\sigma_n^- t.$$

(93)

So again

$$a_n^-(t) = f_n^-(t)a_n^-(0) + g_n^-(t)a_n^{-\dagger}(0).$$

(94)

But now

$$f_n^-(t) = \cosh\sigma_n^- t + \frac{1}{2i\vartheta_n^-}(1 - \vartheta_n^{-2})\sinh\sigma_n^- t,$$

(95)

$$g_n^-(t) = \frac{-1}{2i\vartheta_n^-}(1 + \vartheta_n^{-2})\sinh\sigma_n^- t = \frac{i}{2\vartheta_n^-}\left(\frac{a}{a_{cr}}\right)\frac{\omega_z}{E_n^-}\sinh\sigma_n^- t.$$

(96)

Physically the difference is huge. In the first place, the density is growing exponentially. But unlike the previous case, there is no oscillatory component. While the actual number of particles is increasing, there are no surges in the density caused by the sudden constructive interference of many modes. In particular these particles do not contribute to the central peak in the density distribution. In this sense, they cannot be seen by destructive absorption imaging. Because these particles do not oscillate in the trap, in the sense above, we say these modes are frozen in the same sense used in the theories of cosmological structure formation, i.e., that fluctuations in an evolving universe are said to freeze upon leaving the horizon [44].

However, these modes come alive at τ_{evolve}, when the scattering length is set to zero. Now they become ordinary trap modes, and oscillate in the trap in the same way as the burst described above. To the observer, they appear as a new injection of particles from the core of the condensate, which makes up the so-called jets. The sudden activation of a frozen mode by turning off the particle-particle interaction may be described as a "thaw."

Observe that in this picture several conspicuous features of jets become obvious. Jets may only appear if the turn-off time τ_{evolve} is earlier than the formation of the remnant. Once the condensate is stable again, there are no more frozen modes to thaw. On the other hand, jets will appear (as observed) for $\tau_{evolve} < t_{collapse}$, when the condensate has not yet shed any particles. Also jets must be less energetic than bursts, since they are composed of lower modes. Because of their relative weakness, treating them as test particles riding on the dynamic condensate as is the approximation adopted here ('test field') works better for jets than for bursts. A more accurate depiction of the dynamics of bursts may require consideration of the backreaction of the fluctuations on the condensate.

D. Beyond $t_{collapse}$: Thawing

The main physics we presented in the preceding section is that the amplitude for a normal mode in the excitation (fluctuations) of the condensate evolves as a harmonic oscillator with a complex frequency dictated by the dynamics of the condensate. Parametric amplification (or, in a quantum optics, squeezing) of the fluctuations populates the modes above the condensate, even from a vacuum state originally, manifesting as bursts or jets. Thus in our view the specific phenomena arising from the collapse of a BEC formed from a dilute Bose-Einstein gas arises from the squeezing of (vacuum) fluctuations by the condensate dynamics.

Let us now discuss the behavior of fluctuations beyond $t_{collapse}$, when the number of particles in the condensate, and therefore the instantaneous frequency of the excited modes, become time dependent. As in the preceding Section, we shall assume nevertheless that the condensate remains homogeneous, thereby confining ourselves to the early stages of collapse.

For concreteness, let us assume that the number of particles in the condensate remains constant $N_0 = \bar{N}_0 = 16\,000$ up to $t = t_{collapse} = 3$ ms, and then decays exponentially $N_0(t) = \bar{N}_0 \exp[-(t - t_{collapse})/\tau]$, with $\tau = 6$ ms (see Fig. 4). The mean frequency $\omega = 80$ Hz of the trap corresponds to a temperature $\hbar\omega/k_B = 52.5$ nK. The actual trap frequencies reported in Ref. [1] $\omega_{radial} = 110$ Hz and $\omega_{axial} = 42.7$ Hz correspond to temperatures 28.012 (axial) and 72.162 (radial) nK. These are relatively high with respect to the sample temperature of 3 nK. For this reason the initial number of particles above the condensate is negligible, and we may assume that we are dealing with particle creation from effectively the vacuum. This is the rationale behind calling this process "squeezing of the vacuum." We shall assume the scattering length is brought to $a = 36a_0$. We shall approximate the effect of the condensate on the fluctuations by a constant level shift as in Eq. (69). The best fit to the experimental data is obtained for $\kappa = 0.46$, which is satisfactorily close to the experimental value of 0.55.

Shifting the origin of time to $t_{collapse}$ for simplicity, we write $N_0(t) = \bar{N}_0 \exp(-t/\tau)$. After expanding in trap eigenmodes as in the preceding Section, we obtain the equations
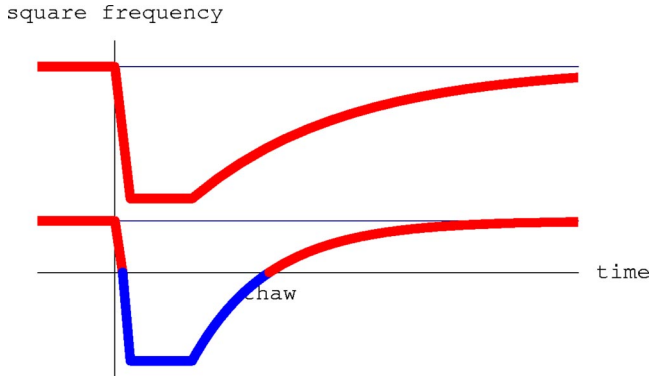
square frequency

FIG. 5. (Color online) A schematic depiction of the evolution of the proper frequencies of different modes in time, both in arbitrary units. Short-wavelength modes remain stable throughout, but the sudden change in proper frequency when the interaction is switched on induces particle creation in them. These particles are perceived as bursts. Long-wavelength modes actually become unstable (or frozen) until the condensate has lost enough atoms. During this period they are amplified. When they become stable again, they are seen as a secondary emission or jet.

$$\frac{d}{dt} b_{\vec{n}} = - \left[E_{\vec{n}} - \left(\frac{a\omega_z}{\bar{a}} \right) \exp(-t/\tau) \right] c_{\vec{n}}, \qquad (97)$$

$$\frac{d}{dt} c_{\vec{n}} = E_{\vec{n}} b_{\vec{n}}. \qquad (98)$$

Therefore

$$\frac{d^2}{dt^2} c_{\vec{n}} + E_{\vec{n}} \left[E_{\vec{n}} - \left(\frac{a\omega_z}{\bar{a}} \right) \exp(-t/\tau) \right] c_{\vec{n}} = 0. \qquad (99)$$

This equation clearly displays the two kinds of behavior described above (an exact solution is provided in Appendix B). If $E_{\vec{n}} > (a\omega_z/\bar{a})$, the mode is always oscillatory. If $E_{\vec{n}} < (a\omega_z/\bar{a})$, the mode is frozen at $t_{collapse}$, but thaws when $\exp(-t/\tau) \sim E_{\vec{n}} \bar{a}/a\omega_z$ (see Fig. 5). During the frozen period, the modes are amplified, but they only contribute to bursts after thaw. If the evolution is interrupted while still frozen, they appear as a jet.

We therefore conclude that the number N_{jet} of particles in a jet at time τ_{evolve} is essentially the total number of particles in all frozen modes at that time. If we write as before

$$a_{\vec{n}}(t) = f_{\vec{n}}(t) a_{\vec{n}}(0) + g_{\vec{n}}(t) a_{\vec{n}}^{\dagger}(0), \qquad (100)$$

then

$$N_{jet}(t) = \sum_{E_{\vec{n}} \leqslant (a\omega_z/\bar{a}) \exp(-t/\tau)} |g_{\vec{n}}(t)^2|. \qquad (101)$$

This is plotted in Fig. 6, from the exact solution in Appendix B, with the parameters given above, and compared to the corresponding results as reported in Ref. [1]. We see that the agreement is excellent at early times (up to about 6 ms). For later times, the model overestimates the jet population. This
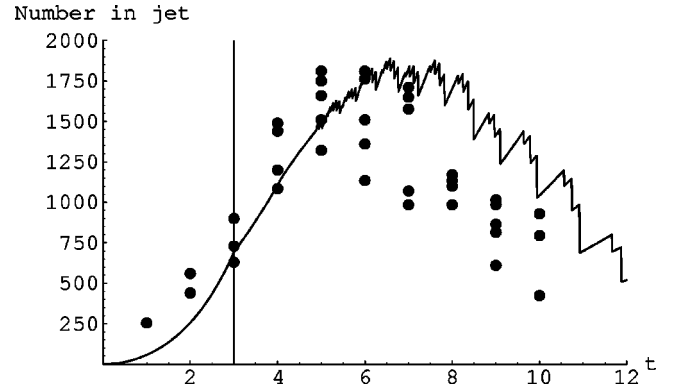
Number in jet

FIG. 6. The evolution of the number of particles in a jet as a function of the time t_{evolve} (measured in milliseconds), for $\bar{N}_0 = 16\,000$, $\omega_{radial} = 110$ Hz, $\omega_{axial} = 42.7$ Hz, $a = 36a_0$, and $\kappa = 0.46$ [see Eq. (69)]. The evolution of $N(t)$ in time is depicted in Fig. 4. To provide a visual reference we have superimposed the data of Fig. 6 of Ref. [1]. The discrepancy between theory and experiment beyond $t_{evolve} = 6$ ms may be attributed to an overestimation of the condensate-noncondensate coupling in neglecting the change in the shape of the condensate.

is due to the fact that, by not considering the shrinking of the condensate, we are overestimating the overlap between the condensate and the fluctuations, thus delaying the thaw. It nevertheless reproduces the overall slope of the particle number with τ_{evolve}, which is quite remarkable considering the simplicity of the model.

The see-saw pattern follows from the discreteness of the modes. Modes thaw at discrete times t_k^*. Between one and the next, occupation numbers of the unstable modes are increasing, and so the number of particles in the jet is a growing function of τ_{evolve}. When the next stabilization occurs, the particles in the now stable mode no longer contribute to later jets, and the particle number in the jet decreases by a finite amount. This pattern accounts for the fact that a jet from a later τ_{evolve} may be stronger than earlier ones, and also for the large variation in the number of particles in jets with similar values of τ_{evolve}. It should also be remembered that we are computing the expected number of particles, but that, in the highly squeezed state which results from the frozen period, the fluctuations in particle number are comparable to the mean number itself.

V. CONCLUSION

In this paper, we have applied insight from the quantum field theory of particle creation and structure formation in cosmological spacetimes and the theory of second-order phase transitions to a specific scenario of controlled collapse of a Bose-Einstein condensate, as observed in the experiment to Donley and co-workers [1,2]. We have described these phenomena as resulting from particle creation from the vacuum, induced by the time-dependent condensate. This time dependence squeezes and amplifies the field operator describing excitations above the condensate. A key concept in our analysis borrowed from theories of cosmological structure formation is the drastic difference in the physical

effects of frozen versus oscillatory modes: those whose physical frequencies are higher than the collapse rate oscillate and are rather impervious to the condensate, while those below (frozen modes) grow in time and get amplified, in a way similar to the growth of fluctuations during spinodal decomposition. As the condensate stabilizes and the collapse rate decreases, the frozen modes begin to thaw. The appearance of oscillatory modes (in second quantized language) is described as particle creation appearing in jets and bursts, as described in detail above.

In order to focus on the key ideas we have adopted a number of simplifying assumptions. We take the condensate evolution as a given input from the experiments, rather than deriving it from fully self-consistent equations. We have treated excitations within the Popov approximation, which improves on the Hartree approach but is known to break down as the number of particles above the condensate increases. We have neglected the coupling between different excitation modes, considering only the coupling of each to the condensate.

These simplifications render certain aspects of the problem more amenable to others because they are rather insensitive to the assumptions. The scaling of $t_{collapse}$ is shown to depend on the behavior of a few modes setting the characteristic time scale of the problem—therefore the prediction is not affected by the underestimation of the coupling to other modes.

Even within these simplifications, we have obtained good quantitative predictions for the onset of instability, the scaling of the waiting time $t_{collapse}$ (when the condensate implosion really begins after the inversion of the scattering length) with the scattering length, and also for the number of particles in a jet as a function of τ_{evolve}, when the interaction between atoms is switched off.

Another success of the model is to provide a simple explanation for the widely different appearance of bursts and jets. As remarked earlier, jets may only appear if the turn-off time τ_{evolve} is earlier than the formation of the remnant, because once the condensate is stable again, there are no more frozen modes to thaw, but, on the other hand, jets will appear for $\tau_{evolve} < t_{collapse}$, when the condensate has not yet shed any particles. Also jets must be less energetic than bursts, since they are composed of lower modes.

Considering the success these simple ideas and light calculations brought about we believe our approach might have captured the essence of the physics behind these phenomena. The physical paradigms we used in bringing forth these ideas also suggest that understanding the basic mechanism of important processes in cosmology, critical dynamics, and Bose-Einstein condensation may share more than a superficial ground.

APPENDIX A: THE CLASSICAL GPE

In this appendix we shall consider the purely classical GPE, meaning that we shall disregard any backreaction from fluctuations. The conclusion of this analysis is that for short times of the order of 1 ms, it is possible to consider the modulus of the condensate as time independent, and its phase as space independent. This observation will lead to a substantial simplification of the equations for the fluctuations in this regime.

Let us begin from the equations

$$\frac{\partial \Theta}{\partial t} + \frac{1}{2}(\boldsymbol{\nabla}\Theta)^2 - \frac{1}{\Phi_0}H\Phi_0 + u\Phi_0^2 = 0, \qquad (A1)$$

$$\frac{\partial \Phi_0}{\partial t} + \boldsymbol{\nabla}\Theta\boldsymbol{\nabla}\Phi_0 + \frac{1}{2}(\boldsymbol{\nabla}^2\Theta)\Phi_0 = 0. \qquad (A2)$$

It is suggestive to rewrite these equations in the following way. The operator

$$D_t = \frac{\partial}{\partial t} + (\boldsymbol{\nabla}\Theta)\boldsymbol{\nabla} \qquad (A3)$$

looks a lot as a material derivative with respect to a fluid flowing at each point with velocity $v = \boldsymbol{\nabla}\Theta$. It seems natural to change from the Eulerian coordinates x to Lagrangian coordinates q. That is, for given q we define the function $x = x(q,t)$ as the solution to the system

$$\left.\frac{\partial x(q,t)}{\partial t}\right|_q = \boldsymbol{\nabla}_x\Theta(x(q,t),t), \quad x(q,0) = q. \qquad (A4)$$

Observe that

$$D_t = \left.\frac{\partial}{\partial t}\right|_q. \qquad (A5)$$

It is also convenient to define the fields

$$J^i_\alpha = \left.\frac{\partial x^i}{\partial q^\alpha}\right| \qquad (A6)$$

and their inverses J^α_i. At any given time, the q^α are a set of curvilinear coordinates, with metric

$$ds^2 = g_{\alpha\beta}dq^\alpha dq^\beta, \qquad (A7)$$

$$g_{\alpha\beta} = \delta_{ij}J^i_\alpha J^j_\beta. \qquad (A8)$$

The wave function transforms as a scalar under this coordinate change. We also define

$$J = \det J^i_\alpha. \qquad (A9)$$

Observe that

$$\frac{\partial J}{\partial t}\bigg|_{q}=JJ_i^{\alpha}\frac{\partial^2\Theta}{\partial q^{\alpha}\partial x^i}=J\nabla^2\Theta. \qquad \text{(A10)}$$

The volume element is $\sqrt{g}d^3q, g=\det g_{\alpha\beta}=J^2$, and the Laplacian

$$\frac{1}{\sqrt{g}}\partial_{\alpha}\sqrt{g}g^{\alpha\beta}\partial_{\beta}. \qquad \text{(A11)}$$

This suggests writing

$$\Phi_0=\frac{\Phi_0}{\sqrt{J}} \qquad \text{(A12)}$$

to get the equation

$$\frac{\partial\Phi_0}{\partial t}=0. \qquad \text{(A13)}$$

Writing the dynamics this way, the role of the phases is hidden in the time dependent curvilinear coordinate system, since we get

$$\Phi_0=\Phi_0(q)=\frac{\sqrt{N_0}}{\pi^{3/4}}e^{-q^2/2}, \qquad \text{(A14)}$$

where we are using the fact that initially the condensate corresponds to a noninteracting gas.

To be definite, consider a situation with $N_0=16\,000$ and $a=30a_0$. We obtain

$$N_0 u=4\pi\frac{a}{a_{ho}}N_0=104. \qquad \text{(A15)}$$

Since we expect that, at least initially, $H\Phi_0\sim 3\Phi_0/2$, the dynamics of the phase near the origin is dominated by the $u\Phi_0^2$ term. Concretely, observe that

$$\frac{\partial\Theta}{\partial t}\bigg|_x=\frac{\partial\Theta}{\partial t}\bigg|_q-(\nabla\Theta)^2. \qquad \text{(A16)}$$

So the equation for the phase reads

$$\frac{\partial\Theta}{\partial t}-\frac{1}{2}(\nabla\Theta)^2-\frac{\sqrt{J}}{\Phi_0}H\frac{\Phi_0}{\sqrt{J}}+\frac{u}{\sqrt{J}}\Phi_0^2=0. \qquad \text{(A17)}$$

Approximate

$$\Theta(q,t)=\mu_0-t\left[u\Phi_0^2(q)-\frac{3}{2}\right]. \qquad \text{(A18)}$$

Observe that

$$\nabla\Theta=2tuq\Phi_0^2(q). \qquad \text{(A19)}$$

So

$$\tfrac{1}{2}(\nabla\Theta)^2=(2t^2uq^2\Phi_0^2(q))u\Phi_0^2(q). \qquad \text{(A20)}$$

This term is therefore negligible against $u\Phi_0^2$ if $q\gg 1$ or $q\leqslant(t\sqrt{N_0 u})^{-1}$; it is small everywhere if $t\leqslant(\sqrt{N_0 u})^{-1}$. This is enough to justify the formal procedures in the main body of this paper.

The equation that defines the coordinate change from x to q becomes

$$\frac{\partial x(q,t)}{\partial t}\bigg|_{q}=2tuq\Phi_0^2(q), \quad x(q,0)=q, \qquad \text{(A21)}$$

with the solution

$$x=q[1+t^2u\Phi_0^2(q)]. \qquad \text{(A22)}$$

So again, we see that during the first millisecond, we may approximate $x=q$ everywhere. This establishes the conclusions anticipated at the beginning of this section.

APPENDIX B: EXACT SOLUTIONS OF THE MODE EQUATION IN THE DYNAMICAL CASE

In this appendix we shall derive closed-form solutions for the evolution equations for quantum fluctuations after $t_{collapse}$,

$$\frac{d}{dt}b_{\vec{n}}=-\left[E_{\vec{n}}-\left(\frac{a\omega_z}{\bar{a}}\right)\exp(-t/\tau)\right]c_{\vec{n}}, \qquad \text{(B1)}$$

$$\frac{d}{dt}c_{\vec{n}}=E_{\vec{n}}b_{\vec{n}}. \qquad \text{(B2)}$$

Therefore

$$\frac{d^2}{dt^2}c_{\vec{n}}+E_{\vec{n}}\left[E_{\vec{n}}-\left(\frac{a\omega_z}{\bar{a}}\right)\exp(-t/\tau)\right]c_{\vec{n}}=0. \qquad \text{(B3)}$$

Call

$$\zeta=\zeta_0 e^{(-t/2\tau)}. \qquad \text{(B4)}$$

Therefore

$$\frac{d}{dt}=\frac{-\zeta}{2\tau}\frac{d}{d\zeta} \qquad \text{(B5)}$$

and

$$\frac{1}{4\tau^2}\zeta\frac{d}{d\zeta}\zeta\frac{d}{d\zeta}c_{\vec{n}}+E_{\vec{n}}\left[E_{\vec{n}}-\left(\frac{a\omega_z}{\bar{a}}\right)\left(\frac{\zeta}{\zeta_0}\right)^2\right]c_{\vec{n}}=0, \qquad \text{(B6)}$$

so

$$\frac{d^2}{d\zeta^2}c_{\vec{n}}+\frac{1}{\zeta}\frac{d}{d\zeta}c_{\vec{n}}-\left(\frac{4\tau^2 a\omega_z E_{\vec{n}}}{\bar{a}\zeta_0^2}-\frac{4\tau^2 E_{\vec{n}}^2}{\zeta^2}\right)c_{\vec{n}}=0. \qquad \text{(B7)}$$

Choose

$$\zeta_0^2=\frac{4\tau^2 a\omega_z E_{\vec{n}}}{\bar{a}} \qquad \text{(B8)}$$

to find (recall that the $c_{\vec{n}}$ are self-adjoint)

$$c_n^- = \alpha_n^- I_{2i\tau E_n^-}(\zeta) + \alpha_n^{\dagger} I_{-2i\tau E_n^-}(\zeta). \quad \text{(B9)}$$

We see the two basic behaviors discussed in the preceding section. For $t \ll \tau$, $\zeta \gg 1$, the Bessel functions behave as real exponentials. When $t \to \infty$, $\zeta \to 0$, the modes oscillate with frequency $\pm E_n^-$. Modes with $E_n^- > a\omega_z/\bar{a}$ are never frozen. Lower modes are frozen at $t = 0$, but thaw when $\zeta \sim 2\tau E_n^-$, or

$$e^{(-t/\tau)} \sim \frac{\bar{a} E_n^-}{a\omega_z}. \quad \text{(B10)}$$

The b_n^- coefficients are given by

$$b_n^- = \frac{1}{E_n^-} \frac{dc_n^-}{dt} = \frac{-\zeta}{2E_n^-\tau} \frac{dc_n^-}{d\zeta}. \quad \text{(B11)}$$

The c_n^- and b_n^- coefficients must be continuous, so

$$\alpha_n^- I_{2i\tau E_n^-}(\zeta_0) + \alpha_n^{\dagger} I_{-2i\tau E_n^-}(\zeta_0) = \bar{c}_n^-, \quad \text{(B12)}$$

$$\frac{-\zeta_0}{2E_n^-\tau}\left[\alpha_n^- \frac{d}{d\zeta} I_{2i\tau E_n^-}(\zeta_0) + \alpha_n^{\dagger} \frac{d}{d\zeta} I_{-2i\tau E_n^-}(\zeta_0)\right] = \bar{b}_n^-, \quad \text{(B13)}$$

where $\bar{c}_n^-$ and $\bar{b}_n^-$ are the results of the evolution up to $t_{collapse}$, namely,

$$\bar{c}_n^- = \frac{1}{2}(a_n^- + a_n^{\dagger})(0)\cosh \sigma_n^- t_{collapse}$$

$$+ \frac{1}{2i} \frac{(a_n^- - a_n^{\dagger})(0)}{\vartheta_n^-}\sinh \sigma_n^- t_{collapse}, \quad \text{(B14)}$$

$$\bar{b}_n^- = \frac{1}{2i}(a_n^- - a_n^{\dagger})(0)\cosh \sigma_n^- t_{collapse}$$

$$+ \frac{1}{2}\vartheta_n^-(a_n^- + a_n^{\dagger})(0)\sinh \sigma_n^- t_{collapse}. \quad \text{(B15)}$$

Using the Wronskian

$$I_{2i\tau E_n^-}(\zeta_0)\frac{d}{d\zeta} I_{-2i\tau E_n^-}(\zeta_0) - I_{-2i\tau E_n^-}(\zeta_0)\frac{d}{d\zeta} I_{2i\tau E_n^-}(\zeta_0)$$

$$= -2i\frac{\sinh 2\pi\tau E_n^-}{\pi\zeta_0}, \quad \text{(B16)}$$

we get

$$\alpha_n^- = \frac{i\pi\zeta_0}{2\sinh 2\pi\tau E_n^-}\left[\frac{d}{d\zeta} I_{-2i\tau E_n^-}(\zeta_0)\bar{c}_n^- + I_{-2i\tau E_n^-}(\zeta_0)\frac{2E_n^-\tau}{\zeta_0}\bar{b}_n^-\right]. \quad \text{(B17)}$$

Call

$$W(\zeta,\zeta_0) = \frac{i\pi\zeta_0}{2\sinh 2\pi\tau E_n^-}[I_{2i\tau E_n^-}(\zeta)I_{-2i\tau E_n^-}(\zeta_0)$$

$$- I_{-2i\tau E_n^-}(\zeta)I_{2i\tau E_n^-}(\zeta_0)], \quad \text{(B18)}$$

$$W_1(\zeta,\zeta_0) = \frac{i\pi\zeta_0}{2\sinh 2\pi\tau E_n^-}\left[I_{2i\tau E_n^-}(\zeta)\frac{d}{d\zeta} I_{-2i\tau E_n^-}(\zeta_0)\right.$$

$$\left. - I_{-2i\tau E_n^-}(\zeta)\frac{d}{d\zeta} I_{2i\tau E_n^-}(\zeta_0)\right], \quad \text{(B19)}$$

$$W_2(\zeta,\zeta_0) = \frac{d}{d\zeta} W(\zeta,\zeta_0), \quad \text{(B20)}$$

$$W_3(\zeta,\zeta_0) = \frac{d}{d\zeta} W_1(\zeta,\zeta_0). \quad \text{(B21)}$$

Then

$$c_n^- = W_1(\zeta,\zeta_0)\bar{c}_n^- + \frac{2E_n^-\tau}{\zeta_0} W(\zeta,\zeta_0)\bar{b}_n^-, \quad \text{(B22)}$$

$$b_n^- = \frac{-\zeta}{2E_n^-\tau}\left[W_3(\zeta,\zeta_0)\bar{c}_n^- + \frac{2E_n^-\tau}{\zeta_0} W_2(\zeta,\zeta_0)\bar{b}_n^-\right], \quad \text{(B23)}$$

$$\bar{c}_n^- = \frac{1}{2}(\bar{a}_n^- + \bar{a}_n^{\dagger}); \quad \bar{b}_n^- = \frac{1}{2i}(\bar{a}_n^- - \bar{a}_n^{\dagger}), \quad \text{(B24)}$$

$$a_n^-(t) = W_1(\zeta,\zeta_0)\bar{c}_n^- + \frac{2E_n^-\tau}{\zeta_0} W(\zeta,\zeta_0)\bar{b}_n^- - \frac{i\zeta}{2E_n^-\tau}\left[W_3(\zeta,\zeta_0)\bar{c}_n^-\right.$$

$$\left. + \frac{2E_n^-\tau}{\zeta_0} W_2(\zeta,\zeta_0)\bar{b}_n^-\right]. \quad \text{(B25)}$$

So, writing

$$\bar{a}_n^- = \bar{f}_n^- a_n^-(0) + \bar{g}_n^- a_n^{\dagger}(0), \quad \text{(B26)}$$

then

$$a_n^-(t) = f_n^-(t)a_n^-(0) + g_n^-(t)a_n^{\dagger}(0), \quad \text{(B27)}$$

$$f_n^-(t) = \frac{1}{2} W_1(\zeta,\zeta_0)(\bar{f}_n^- + \bar{g}_n^{-*}) - \frac{iE_n^-\tau}{\zeta_0} W(\zeta,\zeta_0)(\bar{f}_n^- - \bar{g}_n^{-*})$$

$$- \frac{i\zeta}{4E_n^-\tau} W_3(\zeta,\zeta_0)(\bar{f}_n^- + \bar{g}_n^{-*})$$

$$- \frac{\zeta}{2\zeta_0} W_2(\zeta,\zeta_0)(\bar{f}_n^- - \bar{g}_n^{-*}), \quad \text{(B28)}$$

$$g_n^-(t) = \frac{1}{2} W_1(\zeta,\zeta_0)(\bar{f}_n^{-*} + \bar{g}_n^-) + \frac{iE_n^-\tau}{\zeta_0} W(\zeta,\zeta_0)(\bar{f}_n^{-*} - \bar{g}_n^-)$$

$$- \frac{i\zeta}{4E_n^-\tau} W_3(\zeta,\zeta_0)(\bar{f}_n^{-*} + \bar{g}_n^-)$$

$$+ \frac{\zeta}{2\zeta_0} W_2(\zeta,\zeta_0)(\bar{f}_n^{-*} - \bar{g}_n^-). \quad \text{(B29)}$$

This result is used to build the plot in Fig. 6.

[1] E. Donley *et al.*, Nature (London) **412**, 295 (2001).

[2] N. Claussen, Ph.D. thesis, University of Colorado, 2003 (unpublished)

[3] J. Roberts *et al.*, Phys. Rev. Lett. **81**, 5109 (1998).

[4] S. Cornish *et al.*, Phys. Rev. Lett. **85**, 1795 (2000).

[5] N. Claussen *et al.*, Phys. Rev. Lett. **89**, 010401 (2002).

[6] E. Donley *et al.*, Nature (London) **417**, 529 (2002).

[7] T. Kohler, T. Gasenzer, and K. Burnett, e-print cond-mat/0209100.

[8] S. Kokkelmans and M. Holland, Phys. Rev. Lett. **89**, 180401 (2002).

[9] M. Mackie, K. Suominen, and J. Javainen, Phys. Rev. Lett. **89**, 180403 (2002).

[10] M. Mackie, K. Suominen, and J. Javainen, e-print cond-mat/0209083, Proc. Cool Interact. (to be published).

[11] M. Mackie *et al.*, e-print physics/0210131.

[12] L. Yin and Z. Ning, Phys. Rev. A **68**, 033608 (2003).

[13] N. Claussen *et al.*, e-print cond-mat/0302195.

[14] J. Milstein, C. Menotti, and M. Holland, New J. Phys. **5**, 52.1 (2003).

[15] E. Shuryak, Phys. Rev. A **54**, 3151 (1996).

[16] C. Sackett, H. Stoof, and R. Hulet, Phys. Rev. Lett. **80**, 2031 (1998).

[17] Yu. Kagan, A. Muryshev, and G. Shlyapnikov, Phys. Rev. Lett. **81**, 933 (1998).

[18] L. Berge and J. Juul Rasmussen, e-print physics/0012004.

[19] K. Huang, e-print cond-mat/0110498.

[20] S.K. Adhikari, Phys. Rev. A **66**, 013611 (2002); **66**, 043601 (2002).

[21] H. Saito and M. Ueda, e-print cond-mat/0305242.

[22] C. Savage, N. Robins, and J. Hope, e-print cond-mat/0207308.

[23] V. N. Popov, *Functional Integrals and Collective Excitations* (Cambridge University Press, Cambridge, England, 1987).

[24] A. Griffin, *Excitations in a Bose-Condensed Liquid* (Cambridge University Press, Cambridge, England, 1993).

[25] A. Griffin, Phys. Rev. B **53**, 9341 (1996).

[26] C. Pethick and H. Smith, *Bose-Einstein Condensation in Dilute Gases* (Cambridge University Press, Cambridge, England, 2002).

[27] T. Kohler and K. Burnett, Phys. Rev. A **65**, 033601 (2002).

[28] R. Duine and H. Stoof, e-print cond-mat/0211514.

[29] Yu. Kagan and L. Maksimov, Phys. Rev. A **64**, 053610 (2001).

[30] A. Vardi and M.G. Moore, Phys. Rev. Lett. **89**, 090403 (2002).

[31] V. Yurovsky, Phys. Rev. A **65**, 033605 (2002).

[32] A. Vardi, V. Yurovsky, and J. Anglin, Phys. Rev. A **64**, 063611 (2001).

[33] V.A. Yurovsky, A. Ben-Reuven, and P. Julienne, Phys. Rev. A **65**, 043607 (2002); V. Yurovsky and A. Ben-Reuven, e-print cond-mat/0205267.

[34] J. Rogel-Salazar *et al.*, e-print cond-mat/0110076.

[35] F. de Souza Cruz, M. Pinto, R. Ramos, and P. Sena, Phys. Rev. A **65**, 053613 (2002); D. Barci, E. Fraga, M. Gleiser, and R. Ramos, Physica A **317**, 535 (2003); D.G. Barci, E.S. Fraga, Rudnei O. Ramos, Laser Phys. **12**, 43 (2002); M. Greiner, O. Mandel, T. Hansch, and I. Bloch, e-print cond-mat/0207196.

[36] D. Boyanovsky *et al.*, Ann. Phys. (N.Y.) **300**, 1 (2002); Phys. Rev. D **59**, 125009 (1999).

[37] K. Góral, M. Gajda, and K. Rzazewski, Phys. Rev. Lett. **86**, 1397 (2001).

[38] A. Csordas, R. Graham, and P. Szepfalusy, Phys. Rev. A **56**, 5179 (1997).

[39] J. Schwinger, Phys. Rev. **82**, 664 (1951).

[40] L. Parker, Phys. Rev. **183**, 1057 (1969)

[41] Ya. B. Zel'dovich, Pis'ma Zh. Éksp. Teor. Fiz **12**, 443 (1970) [JETP Lett. **12**, 307 (1970)]; Y.B. Zel'dovich and A.A. Starobinsky, Zh. Éksp. Teor. Fiz. **61**, 2161 (1971) [Sov. Phys. JETP **34**, 1159 (1971)]; Ya. B. Zel'dovich, in *Magic without Magic: John Archibald Wheeler*, edited by J. Klauder (Freeman, San Francisco, 1973).

[42] L. Grischuk and Y.V. Sidorov, Phys. Rev. D **42**, 3413 (1990); B.L. Hu, G. Kang, and A. Matacz, Int. J. Mod. Phys. A **9**, 991 (1994); K. Koks, A. Matacz, and B.L. Hu, Phys. Rev. D **55**, 5917 (1997).

[43] C. Barcelo, S. Liberati, and M. Visser, Int. J. Mod. Phys. **A18**, 3735 (2003); Class. Quantum Grav. **18**, 1137 (2001); T. Jacobson and T. Koike, in *Artificial Black Holes*, edited by M. Novello, M. Visser, and G. Volovik (World Scientific, Singapore, 2002).

[44] A. A. Starobinsky, in *Field Theory, Quantum Gravity and Strings*, edited by H. J. de Vega and N. Sánchez (Springer-Verlag, Berlin, 1986); B. L. Hu, J. P. Paz, and Y. Zhang, in *The Origin of Structure in the Universe*, Conference at Chateau du Pont d'Oye, Belgium, 1992, edited by E. Gunzig and P. Nardone (Plenum Press, New York, 1993), p. 227 (NATO ASI Series); E. Calzetta and B.L. Hu, Phys. Rev. D **52**, 6770 (1995); C. Kiefer, D. Polarski, and A.A. Starobinsky, Int. J. Mod. Phys. D **7**, 455 (1998).

[45] J.M. Bardeen, Phys. Rev. D **22**, 1882 (1980); V.F. Mukhanov and H.A. Feldman, and R.H. Brandenberger, Phys. Rep. **215**, 203 (1992).

[46] E. Calzetta, Ann. Phys. (N.Y.) **190**, 32 (1989); F. Cooper, Y. Kluger, E. Mottola, and J.P. Paz, Phys. Rev. D **51**, 2377 (1995); R.J. Rivers, e-print cond-mat/0105171, J. Low Temp. Phys. (to be published).

[47] H. Stoof, J. Low Temp. Phys. **114**, 11 (1999).

[48] R. Duine and H. Stoof, Phys. Rev. A **65**, 013603 (2001).

[49] C. Gardiner and P. Zoller, Phys. Rev. A **61**, 033601 (2000).

[50] C. Gardiner, J. Anglin, and T. Fudge, e-print cond-mat/0112129

[51] W. Zurek, Nature (London) **382**, 297 (1996); Phys. Rep. **276**, 178 (1996); G.E. Volovik, in *Artificial Black Holes*, edited by M. Novello, M. Visser, and G. Volovik (World Scientific, Singapore, 2002); G.E. Volovik, J. Low Temp. Phys. **124**, 25 (2001).

[52] J. Roberts *et al.*, Phys. Rev. Lett. **86**, 4211 (2001).

[53] A. Gammal, T. Frederico, and L. Tomio, Phys. Rev. A **64**, 055602 (2001).

[54] M. Trippenbach, Y. Band, and P. Julienne, Phys. Rev. A **62**, 023608 (2000).

[55] R. Wynar *et al.*, Science **287**, 1016 (2000).

[56] S. Kokkelmans (private communication).